

Nowhere to hide: closing in on cosmological homogeneity

James P. Zibin^{1,*} and Adam Moss^{2,†}

¹*Department of Physics & Astronomy
University of British Columbia, Vancouver, BC, V6T 1Z1 Canada*

²*Centre for Astronomy & Particle Theory
University of Nottingham, University Park, Nottingham, NG7 2RD, U.K.*

(Dated: November 12, 2018)

Homogeneity is a crucial, but poorly tested, assumption in cosmology. We introduce a new approach which allows us to place limits on the presence of localized structures within essentially our entire observable volume, using cosmic microwave background secondary anisotropies. We find that structures cannot exceed roughly 20 times their expected amplitude over most of our observable volume. Similarly, we place tight constraints on *statistical* inhomogeneity within our volume, performing the first power spectrum reconstruction using secondary anisotropies alone. We find that the standard model passes this important new consistency test. Our approach probes homogeneity over vastly larger volumes and scales than previous studies based on surveys.

PACS numbers: 98.70.Vc, 98.80.Es, 98.80.Jk

INTRODUCTION

The standard Λ cold dark matter (Λ CDM) cosmological model rests upon a few essential foundations. First, it assumes that Einstein’s general relativity (GR) is valid. Second, it takes the matter content to be a mixture of radiation, baryons, and CDM, together with a cosmological constant. Finally, it adopts the cosmological principle, namely, that the Universe approaches homogeneity and isotropy on the largest scales, and also assumes that the primordial fluctuations are *statistically* homogeneous and isotropic. The first two foundations have been intensively examined, via modified gravity models (see, e.g., [1] for a review) and via dark energy models (see [2, 3] for reviews) and non-standard neutrino and dark matter content.

However, the assumption of homogeneity has received considerably less critical examination. One reason for this is the familiar textbook argument (see, e.g., [4]) that homogeneity is implied by isotropy of the spacetime [sometimes taken to be implied by isotropy of the cosmic microwave background (CMB) [5]] together with the assumption of the Copernican principle (so that the Universe appears isotropic to *all* observers) [6]. But we can circumvent this argument in two ways. First, if we allow for violations of the Copernican principle, then *radial* inhomogeneity centred on us will still be consistent with isotropy. Such models received considerable interest in recent years as alternatives to accelerating models (see, e.g., [7] for a review), although ultimately were unsuccessful when confronted with a variety of observational probes [8–15]. However, more subtle radial inhomogeneity may still bias the determination of cosmological parameters [16–20]. Nevertheless, we will not consider anti-Copernican models in this paper.

The second way to allow for inhomogeneity is to simply note that the CMB (and our spacetime) is *not*, of

course, perfectly isotropic; rather, it contains fluctuations on many scales with amplitudes of order 10^{-5} . Therefore inhomogeneities (beyond those expected in Λ CDM) may be present between us and our last scattering surface (LSS) if they produce sufficiently weak secondary CMB anisotropies [21]. The question then becomes: how large might such inhomogeneities be, without producing *obvious* signs in the CMB? This is a central question that we address in this paper. Clearly, the implications of any such violations of homogeneity could be profound.

Consistency between observations and homogeneity has been examined before, but almost always using surveys to map large-scale structure (see, e.g., [22–28]). These studies have been consistent with homogeneity; claims of anomalously large structures [29, 30] have subsequently been refuted [31–33]. However, current galaxy surveys reach only to redshifts $z \simeq 1$, hence sampling only $\sim 1\%$ of our observable comoving volume. Limited sky coverage further reduces this volume. Some studies [34–38] have used CMB data to constrain particular inhomogeneous or anisotropic models, usually Bianchi models. Ref. [18] used multiple probes to constrain inhomogeneity, but only considered radial structures, i.e., tested for violations of the Copernican principle.

The goal of this paper is to extend the range of scales and redshifts sampled by surveys to test homogeneity over most of our observable volume, using the secondary CMB probes of the integrated Sachs-Wolfe (ISW) effect, the kinetic Sunyaev-Zeldovich (kSZ) effect, the Rees-Sciama (RS) effect, and CMB lensing, as well as galaxy lensing [39]. To do this we must choose parameterizations for the inhomogeneities. We consider spherical structures (motivated by various models for inflationary artifacts [40–42]) and a statistically inhomogeneous power spectrum (motivated by hints of large-scale CMB power asymmetries [43, 44]). Constraints in the latter case amount to a CMB-secondary-based primordial

power spectrum reconstruction. In both cases we consider an otherwise standard Λ CDM universe with *Planck* best-fit parameters [45]. Note that our goal is *not* to perform a targeted search for structures, as has been done for particular inflationary relics [42, 46]. Instead, we wish to place upper limits on the amplitudes of structures that would be *undetectable* against the CMB fluctuations, and hence place limits on allowed departures from homogeneity.

COSMOLOGICAL PROBES

Our primary goal in this paper is to constrain homogeneity over the largest volumes accessible to us. To do this, we must use probes which reach as far as possible. Ideally, we would also prefer methods sensitive to total matter (i.e., metric) fluctuations, to avoid bias uncertainties. The ISW, kSZ, RS, and CMB and galaxy lensing probes satisfy these criteria to various degrees.

To characterize the usefulness of these various observations, we will express their power spectra as line-of-sight integrals in the Limber approximation [47]. First, the ISW spectrum can be written

$$\ell^2 C_\ell^{\text{ISW}} \simeq \frac{72\pi^2}{25\ell} \int_0^{r_{\text{LS}}} dr r g'^2(r) \mathcal{P}_{\mathcal{R}}\left(\frac{\ell}{r}\right) T^2\left(\frac{\ell}{r}\right). \quad (1)$$

Here r_{LS} is the comoving radius to the LSS, g the Λ growth suppression factor, $\mathcal{P}_{\mathcal{R}}(k)$ the (dimensionless) primordial comoving curvature spectrum, $T(k)$ the (linear) transfer function accounting for the suppression during radiation domination, k the comoving wavenumber, and a prime indicates a conformal time derivative.

Similarly, we can write the CMB lensing potential power spectrum in the Limber approximation as [48]

$$\ell^4 C_\ell^\phi \simeq \frac{72\pi^2 \ell}{25} \int_0^{r_{\text{LS}}} dr r \left(\frac{r_{\text{LS}} - r}{r_{\text{LS}} r}\right)^2 g^2(r) \mathcal{P}_{\mathcal{R}}\left(\frac{\ell}{r}\right) T^2\left(\frac{\ell}{r}\right). \quad (2)$$

Finally, the galaxy lensing convergence power spectrum for sources at a single distance r_s becomes (see, e.g., [49])

$$\ell^2 C_\ell^\kappa \simeq \frac{18\pi^2 \ell^3}{25} \int_0^{r_s} dr r \left(\frac{r_s - r}{r_s r}\right)^2 g^2(r) \mathcal{P}_{\mathcal{R}}\left(\frac{\ell}{r}\right) T^2\left(\frac{\ell}{r}\right). \quad (3)$$

To get an idea of the sensitivity of these probes to the scales and redshifts of fluctuations, we plot in Fig. 1 the kernels of Eqs. (1)–(3) in the k - r plane, together with the regions sampled by galaxy surveys and measurements of the primary CMB [50]. For galaxy lensing we choose $r_s = r(z = 1)$. It is clear from this plot that current galaxy surveys sample only a small fraction of the comoving distance to last scattering, and also are insensitive to the largest two decades of length scales that are in principle observable. Similarly, while the primary CMB samples a large range of scales, it is sensitive to distances very close

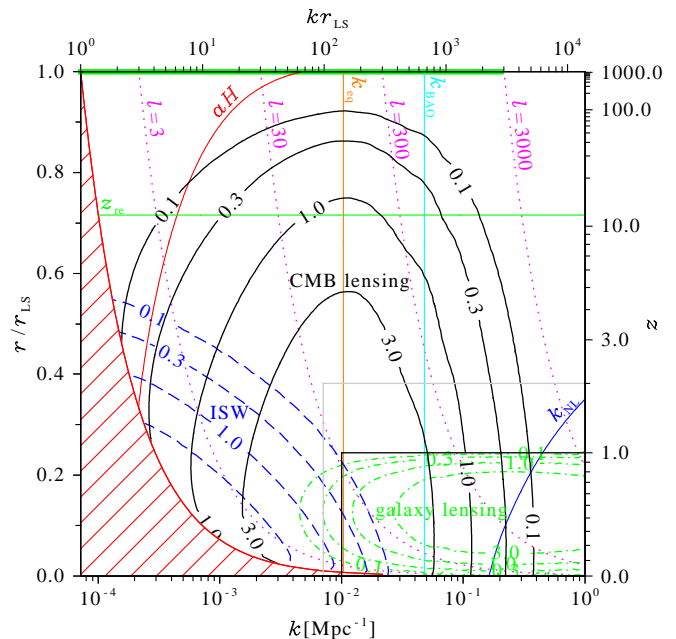


FIG. 1: Limber approximation kernels for the CMB lensing potential (solid black contours), ISW effect (dashed blue contours), and galaxy lensing (dot-dashed green contours). Normalization is arbitrary. The dotted magenta curves indicate the corresponding Limber multipole scale, $\ell = kr$. Scales labelled aH , k_{eq} , k_{BAO} , and k_{NL} are, respectively, the comoving Hubble scale, the equality scale, the first baryon acoustic oscillation peak, and the nonlinearity scale, beyond which information is harder to extract. Geometry prevents measurements in the hatched region (delimited roughly by $\ell = 1$). The black box roughly indicates the range accessed by the WigglyZ survey [27, 51], the grey box by the proposed Euclid survey [52], and the heavy green line by primary CMB.

to last scattering ($r_{\text{LS}} - r \lesssim r_{\text{LS}}/1000$). Therefore, to the extent that galaxy surveys and primary CMB have been utilized to test homogeneity, there is much more room for departures from homogeneity to “hide”. In particular, modifications to the matter power spectrum or localized structures on scales $10^{-4} \text{ Mpc}^{-1} < k < 10^{-2} \text{ Mpc}^{-1}$, or inhomogeneities at $1 \lesssim z \lesssim 1000$ are possible while maintaining consistency with surveys and primary CMB. Any such power spectrum modifications must be localized away from the LSS for consistency with the primary CMB, so they would entail a breaking of statistical homogeneity. Figure 1 makes it apparent that ISW and especially CMB lensing are the most promising probes of the region not accessible to galaxy surveys.

LOCALIZED STRUCTURES

Next we consider the matter of constraining localized structures that may be “lurking” outside the reach of surveys but inside our LSS. We will see that even some *nonlinear* structures will be allowed, so we will treat

the structure with exact GR. We use the spherically symmetric Λ -Lemaître-Tolman-Bondi (ALTB) spacetime [53], sourced by dust and Λ , to represent the standard Λ CDM background with superposed spherical structure [54]. We choose a compensated underdensity with ALT B curvature function profile (in the notation of [11])

$$K(r) = K_0 \left[2 \left(\frac{r}{R} \right)^5 - 3 \left(\frac{r}{R} \right)^4 + \left(\frac{r}{R} \right)^2 \right], \quad (4)$$

with amplitude K_0 and comoving radius R . The ISW, RS, and SW temperature anisotropies due to the structure are calculated by evolving null geodesics from the observer to the LSS, as described in [11, 55]. The deflection angles, α , are translated into lensing potential, ϕ , via $\alpha = \nabla\phi$. The ALT B solution is calculated by numerically evolving Einstein’s equations using independent formulations as checks, including that described in [56]. We also monitor the constraints and compare with LTB and linear theory in the appropriate regimes. The kSZ anisotropies are calculated using linear theory (with reionization width $\Delta z = 0.5$), which we confirm to be in good agreement with the much more time-consuming ALT B kSZ calculation where the kSZ signal dominates. We calculate only the kSZ effect due to the structure itself, not to smaller superimposed structures.

We vary the observer’s position, r , and the structure’s radius. For each pair (R, r) , we iterate to find the amplitude K_0 that results in unity S/N of the structure against the CMB fluctuations, where

$$\left(\frac{S}{N} \right)^2 = \sum_{\ell m} \frac{|a_{\ell m}^T|^2}{C_\ell^T} + \sum_{\ell m} \frac{|a_{\ell m}^\phi|^2}{C_\ell^\phi + N_\ell}. \quad (5)$$

Here $a_{\ell m}^T$ and $a_{\ell m}^\phi$ are the temperature and lensing potential multipoles due to the structure, C_ℓ^T and C_ℓ^ϕ are the standard Λ CDM power spectra, and N_ℓ is the *Planck* lensing reconstruction noise [57]. The temperature contribution is summed over $2 \leq \ell \leq 2000$, while for lensing we restrict the sum to $40 \leq \ell \leq 400$, corresponding to the range reliably measured by *Planck* [58, 59].

The results are presented in Fig. 2, where the colour values indicate the structure amplitude required to give a total S/N of unity. The plotted value is the ratio of the perturbation amplitude, \mathcal{R} , to the amplitude *expected* in Λ CDM, $\mathcal{P}_{\mathcal{R}}^{1/2}(R^{-1})$ [60]. Thus a colour value of, e.g., 10 at some (R, r) means that a structure at that distance and radius must have an amplitude less than 10 times the expected Λ CDM value in order to be undetectable against the CMB. Comparing Figs. 2 and 1, we can see that we have tighter constraints in the regions corresponding to the ISW and CMB lensing, and, as expected, very tight constraints close to the LSS, where the SW effect dominates. (Note that we can roughly relate $k \simeq 2\pi/R$.) A wedge near reionization shows that the kSZ is a strong constraint there. The majority of the

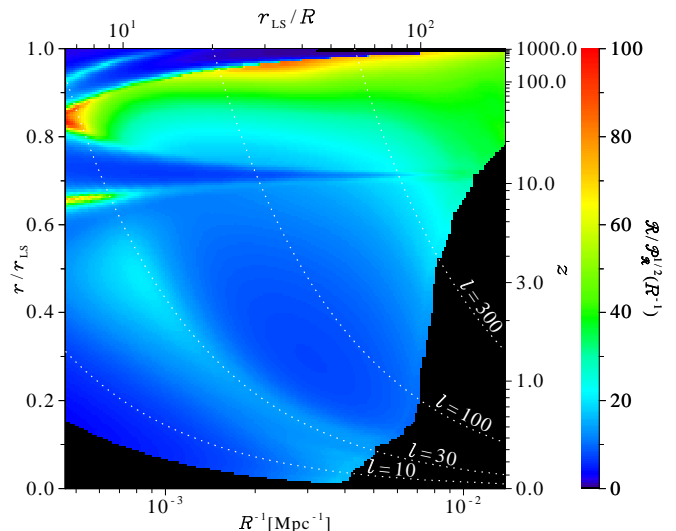


FIG. 2: Largest undetectable amplitude for localized structures relative to the expected Λ CDM amplitude. The structures’ approximate peak multipole scales are also indicated. Constraints are tightest (blue regions) near $r = r_{\text{LS}}$ (due to the SW effect), near reionization (kSZ), in the lower left corner (ISW), and in the centre (CMB lensing plus subdominant RS). In the black area at the bottom the observer would be inside the structure, and in the black area at right shell crossings occur before $S/N = 1$ is reached.

(R, r) plane is constrained most tightly by CMB lensing. Some of the parameter space is untestable with the ALT B model since the structures become so strongly nonlinear that shell crossings occur before $S/N = 1$ is reached.

The “kSZ wedge” has an interesting interpretation: the kSZ effects due to the near and far sides of structures entirely at $z < z_{\text{re}}$, for reionization at z_{re} , approximately cancel. For structures centred near z_{re} , however, very little kSZ is generated at the far side, so there is no cancellation, leading to strong constraints along the wedge.

Figure 2 shows at a glance how large the amplitude can be for structures that are hiding in our observable volume, as a function of size and distance, and in particular outside the region of parameter space directly sampled with galaxy surveys. For example, a 1 Gpc-radius structure halfway to our LSS with as much as 15 times the expected Λ CDM amplitude would go unnoticed [61].

Repeating our calculations for an *overdensity* with profile (4), we find very small differences due to the change in sign between the RS and other anisotropies. Underdensities with the non-compensated profile from [9] result in somewhat weaker constraints in some areas and stronger constraints in others, with the broad picture unchanged.

STATISTICAL INHOMOGENEITY

Next we address the limits that can be placed on statistical inhomogeneity from CMB secondaries as well

as galaxy lensing data. Our approach is to constrain separately the primordial spectrum using primary anisotropies at $z > 100$, $\mathcal{P}_{\mathcal{R}}^{\text{LS}}(k)$, and the primordial spectrum using secondaries and galaxy lensing at $z \leq 100$, $\mathcal{P}_{\mathcal{R}}^{\text{in}}(k)$. As Fig. 1 shows, $z = 100$ separates reasonably well the primary and secondary sources. The last scattering (LS) spectrum is parameterized as usual by $\mathcal{P}_{\mathcal{R}}^{\text{LS}}(k) = A_{\text{S}}(k/k_0)^{n_{\text{S}}-1}$ (with pivot scale $k_0 = 0.05 \text{ Mpc}^{-1}$). We parameterize $\mathcal{P}_{\mathcal{R}}^{\text{in}}(k)$ by a cubic spline, choosing 7 knots a decade apart from $k = 10^{-5}$ to 10 Mpc^{-1} , so all observable scales are well within this range. Our approach is sensitive to statistical inhomogeneity, with different primordial spectra inside versus at the LSS, and serves as a consistency test for ΛCDM .

The data we use are: the CMB temperature power spectrum measured by *Planck* [45], with polarization and temperature-polarization (*TE*) cross-correlation power spectra for $\ell \leq 32$ from the WMAP9 release [62]; the *Planck* lensing potential power spectrum [58]; and the 2D cosmic shear signal measured by the Canada-France-Hawaii Telescope Lensing Survey [63]. We restrict the shear signal to linear scales by imposing an angular cut of $\theta_c = 17'$ and $53'$ for the ξ^+ and ξ^- correlation functions, respectively (see [63] for details). The Markov-Chain-Monte-Carlo fitting methodology requires some modification with our approach: the transfer functions and power spectrum are computed twice, once restricting the source functions to $z > 100$ and once to $z \leq 100$, and each component of the total likelihood is then given the appropriate spectrum. This approach works insofar as one can isolate the observables to each redshift range: this is a good approximation, apart from the *lensed* primary temperature power spectrum at high ℓ . We take $\mathcal{P}_{\mathcal{R}}^{\text{LS}}(k)$ to smooth the primary CMB spectrum, so our results are conservative by neglecting any modification to this. Note that *ISW*, reconstructed lensing potential, and galaxy lensing *are* modified by the interior power spectrum $\mathcal{P}_{\mathcal{R}}^{\text{in}}(k)$. Also, note that we automatically include the (large-scale) *kSZ* effect via the Boltzmann evolution.

The results of our analysis are illustrated in Fig. 3, where we show the 1 and 2σ confidence intervals of the LS and interior primordial power spectra. Unsurprisingly, the LS spectrum is more tightly constrained, although the errors would increase somewhat if the power law assumption was relaxed. The interior spectrum is consistent with the LS spectrum, and is constrained quite well in the range $k \simeq 0.008$ to 0.2 Mpc^{-1} , precisely the scales probed by CMB and galaxy lensing. Larger scales are more weakly constrained by CMB lensing, *ISW*, and *TE* polarization. $\mathcal{P}_{\mathcal{R}}^{\text{in}}(k)$ is pulled down relative to $\mathcal{P}_{\mathcal{R}}^{\text{LS}}(k)$ by the galaxy lensing data on small scales and pushed up by CMB lensing on larger scales. One consequence of the additional freedom in $\mathcal{P}_{\mathcal{R}}^{\text{in}}(k)$ is an increase in the errors on other cosmological parameters. With only *TE* data, e.g., the optical depth to reionization, τ , would be completely degenerate with A_{S} . However, this degeneracy is

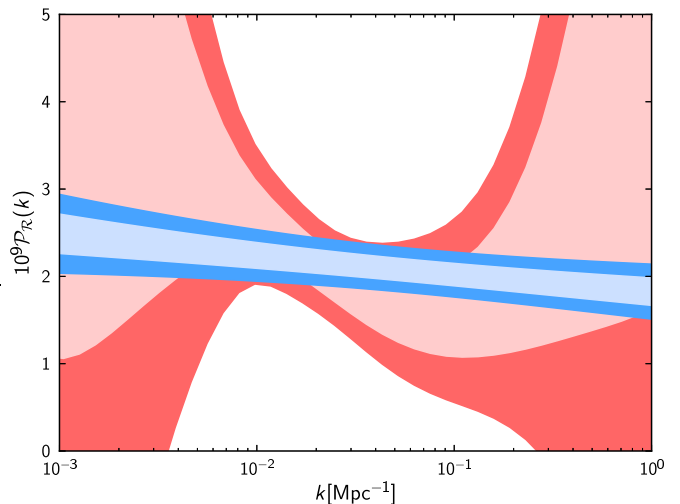


FIG. 3: 1 and 2σ confidence intervals of the primordial spectrum $\mathcal{P}_{\mathcal{R}}^{\text{LS}}(k)$ for $z > 100$ (blue) and $\mathcal{P}_{\mathcal{R}}^{\text{in}}(k)$ for $z \leq 100$ (red).

broken with the inclusion of temperature data, and we find $\tau = 0.06 \pm 0.03$.

CONCLUSIONS

The results in this paper represent our first quantitative look at what might be “hiding” in most of our observable volume. Figure 2 quantifies how large departures from homogeneity, in the form of spherical structures, are allowed by current data. In particular, CMB lensing (and to a lesser extent *ISW* and *kSZ*) restrict structures over most of our observable volume to $\lesssim 20$ times the ΛCDM amplitude. We also find that, while the *ISW* effect is a good probe of very large scales at late times, CMB lensing is unmatched in its ability to inform us about most of the visible Universe and a wide range of scales.

Similarly, Fig. 3 illustrates our current ability to constrain statistical inhomogeneity in the fluctuation spectrum which affects the secondary but not the primary CMB. Equivalently, this represents the first power spectrum reconstruction based on CMB secondaries alone. ΛCDM has passed an important new consistency test.

There are many possibilities for followup work. For localized structures, the assumption of spherical symmetry could be relaxed using linear perturbation theory, at least outside the region of parameter space where nonlinear structures are allowed. For statistical inhomogeneity, there is clearly much freedom in how to parameterize the interior power spectrum, since not only could the radial distribution be modified, but non-trivial angular dependence should be considered as well (motivated, perhaps, by suggestions of a dipolar CMB power asymmetry [44] that would actually extend to our LSS).

In the near future, we can expect improved CMB lensing measurements from the South Pole Telescope, and

also from *Planck* with the availability of the full mission data, including polarization. Farther ahead, we can hope that information about fluctuations over very large distances can be retrieved from remote CMB quadrupole measurements [64] or from other potential probes [7, 65]. Ultimately, we can anticipate that surveys will again take the lead, as 21-cm measurements may map most of our observable volume [66] and provide a nearly complete picture of our patch of the Universe.

Acknowledgments

We thank D. Hanson for assistance with the *Planck* lensing data and D. Scott for comments on the draft. This research was supported by the Canadian Space Agency and the STFC. We acknowledge the use of the CAMB [67] and COSMOMC [68] codes.

* Electronic address: zibin@phas.ubc.ca

† Electronic address: adam.moss@nottingham.ac.uk

- [1] T. Clifton, P. G. Ferreira, A. Padilla, and C. Skordis, *Phys. Rept.* **513**, 1 (2012), arXiv:1106.2476 [astro-ph.CO].
- [2] E. J. Copeland, M. Sami, and S. Tsujikawa, *Int. J. Mod. Phys. D* **15**, 1753 (2006), arXiv:hep-th/0603057.
- [3] M. Li, X.-D. Li, S. Wang, and Y. Wang, *Commun. Theor. Phys.* **56**, 525 (2011), arXiv:1103.5870 [astro-ph.CO].
- [4] R. M. Wald, *General Relativity* (University of Chicago Press, Chicago, 1984).
- [5] Note that the connection between isotropy of the CMB and isotropy of the spacetime is not trivial (see, e.g., [65]).
- [6] Another reason is the theoretical bias that we expect inflation to homogenize and isotropize the Universe, leaving only the fluctuations generated by inflation.
- [7] C. Clarkson, *Comptes Rendus Physique* **13**, 682 (2012), arXiv:1204.5505 [astro-ph.CO].
- [8] T. Biswas, A. Notari, and W. Valkenburg, *JCAP* **1011**, 030 (2010), arXiv:1007.3065 [astro-ph.CO].
- [9] A. Moss, J. P. Zibin, and D. Scott, *Phys. Rev. D* **83**, 103515 (2011), arXiv:1007.3725 [astro-ph.CO].
- [10] P. Zhang and A. Stebbins, *Phys. Rev. Lett.* **107**, 041301 (2011), arXiv:1009.3967 [astro-ph.CO].
- [11] J. P. Zibin, *Phys. Rev. D* **84**, 123508 (2011), arXiv:1108.3068 [astro-ph.CO].
- [12] P. Bull, T. Clifton, and P. G. Ferreira, *Phys. Rev. D* **85**, 024002 (2012), arXiv:1108.2222 [astro-ph.CO].
- [13] M. Zumalacarregui, J. Garcia-Bellido, and P. Ruiz-Lapuente, *JCAP* **1210**, 009 (2012), arXiv:1201.2790 [astro-ph.CO].
- [14] P. Ade et al. (Planck Collaboration), *Astron. Astrophys.* (2013), arXiv:1303.5090 [astro-ph.CO].
- [15] M. Redlich, K. Bolejko, S. Meyer, G. F. Lewis, and M. Bartelmann (2014), arXiv:1408.1872 [astro-ph.CO].
- [16] T. M. Davis, L. Hui, J. A. Frieman, T. Haugbolle, R. Kessler, et al., *Astrophys. J.* **741**, 67 (2011), arXiv:1012.2912 [astro-ph.CO].
- [17] W. Valkenburg and O. E. Bjaelde, *Mon. Not. Roy. Astron. Soc.* **424**, 495 (2012), arXiv:1203.4567 [astro-ph.CO].
- [18] W. Valkenburg, V. Marra, and C. Clarkson, *Mon. Not. Roy. Astron. Soc.* **438**, L6 (2014), arXiv:1209.4078 [astro-ph.CO].
- [19] W. Valkenburg, M. Kunz, and V. Marra (2013), arXiv:1302.6588 [astro-ph.CO].
- [20] R. Wojtak, A. Knebe, W. A. Watson, I. T. Iliev, S. Hess, et al. (2013), arXiv:1312.0276 [astro-ph.CO].
- [21] We assume the Copernican principle, eliminating anomalously large radial inhomogeneity, but we do *not* assume that all observers would see a similarly isotropic CMB, as was done in [7, 37, 65]. This means that we allow for anomalously large inhomogeneities, as long as we are positioned randomly with respect to them. The stronger condition used in [7, 37, 65] would exclude such structures, since they would intersect the last scattering surface of *some* observer, producing a strongly anisotropic CMB for that observer.
- [22] D. W. Hogg, D. J. Eisenstein, M. R. Blanton, N. A. Bahcall, J. Brinkmann, et al., *Astrophys. J.* **624**, 54 (2005), arXiv:astro-ph/0411197.
- [23] J. Yadav, S. Bharadwaj, B. Pandey, and T. Shadri, *Mon. Not. Roy. Astron. Soc.* **364**, 601 (2005), arXiv:astro-ph/0504315.
- [24] P. Sarkar, J. Yadav, B. Pandey, and S. Bharadwaj, *Mon. Not. Roy. Astron. Soc.* **399**, L128 (2009), arXiv:0906.3431 [astro-ph.CO].
- [25] C. M. Hirata, *JCAP* **0909**, 011 (2009), arXiv:0907.0703 [astro-ph.CO].
- [26] C. Marinoni, J. Bel, and A. Buzzi, *JCAP* **1210**, 036 (2012), arXiv:1205.3309 [astro-ph.CO].
- [27] M. Scrimgeour, T. Davis, C. Blake, J. B. James, G. Poole, et al., *Mon. Not. Roy. Astron. Soc.* **425**, 116 (2012), arXiv:1205.6812 [astro-ph.CO].
- [28] B. Hoyle, R. Tojeiro, R. Jimenez, A. Heavens, C. Clarkson, et al., *Astrophys. J.* **762**, L9 (2012), arXiv:1209.6181 [astro-ph.CO].
- [29] R. K. Sheth and A. Diaferio, *Mon. Not. Roy. Astron. Soc.* **417**, 2938 (2011), arXiv:1105.3378 [astro-ph.CO].
- [30] R. G. Clowes, K. A. Harris, S. Raghunathan, L. E. Campusano, I. K. Soechting, et al., *Mon. Not. Roy. Astron. Soc.* **429**, 2910 (2013), arXiv:1211.6256 [astro-ph.CO].
- [31] C. Park, Y.-Y. Choi, J. Kim, I. Gott, J. Richard, S. S. Kim, et al., *Astrophys. J.* **759**, L7 (2012), arXiv:1209.5659 [astro-ph.CO].
- [32] S. Nadathur, *Mon. Not. Roy. Astr. Soc.* **434**, 398 (2013), arXiv:1306.1700 [astro-ph.CO].
- [33] S. Pilipenko and A. Malinovsky (2013), arXiv:1306.3970 [astro-ph.CO].
- [34] E. Martínez-González and J. L. Sanz, *Astron. Astrophys.* **300**, 346 (1995).
- [35] E. F. Bunn, P. Ferreira, and J. Silk, *Phys. Rev. Lett.* **77**, 2883 (1996), arXiv:astro-ph/9605123.
- [36] A. Kogut, G. Hinshaw, and A. Banday, *Phys. Rev. D* **55**, 1901 (1997), arXiv:astro-ph/9701090.
- [37] W. R. Stoeger, M. Araujo, and T. Gebbie, *Astrophys. J.* **476**, 435 (1997), arXiv:astro-ph/9904346.
- [38] P. Ade et al. (Planck Collaboration) (2013), arXiv:1303.5086 [astro-ph.CO].
- [39] Note that homogeneity is technically a property of space-like slices of a spacetime, while the observations we use in this paper probe the surface of our past light cone.

Therefore, we must specify the spacetime *evolution* in order to connect the light cone with some spacelike slice. We assume GR, although for our purposes this subtlety is irrelevant since it appears very likely that a very large structure at $z = 5$, e.g., would result in inhomogeneous slices (today, e.g.) for *any* reasonable evolution law.

- [40] A. Fialkov, N. Itzhaki, and E. D. Kovetz, JCAP **1002**, 004 (2010), arXiv:0911.2100 [astro-ph.CO].
- [41] N. Afshordi, A. Slosar, and Y. Wang, JCAP **1101**, 019 (2011), arXiv:1006.5021 [astro-ph.CO].
- [42] G. Aslanyan, A. V. Manohar, and A. P. Yadav, JCAP **1302**, 040 (2013), arXiv:1301.5641 [astro-ph.CO].
- [43] H. Eriksen, F. Hansen, A. Banday, K. Gorski, and P. Lilje, Astrophys. J. **605**, 14 (2004), arXiv:astro-ph/0307507.
- [44] P. Ade et al. (Planck Collaboration) (2013), arXiv:1303.5083 [astro-ph.CO].
- [45] P. Ade et al. (Planck Collaboration) (2013), arXiv:1303.5076 [astro-ph.CO].
- [46] S. M. Feeney, M. C. Johnson, J. D. McEwen, D. J. Mortlock, and H. V. Peiris, Phys. Rev. **D88**, 043012 (2013), arXiv:1210.2725 [astro-ph.CO].
- [47] D. N. Limber, Astrophys. J. **117**, 134 (1953).
- [48] A. Lewis and A. Challinor, Phys. Rept. **429**, 1 (2006), arXiv:astro-ph/0601594.
- [49] D. Huterer, Phys. Rev. **D65**, 063001 (2002), arXiv:astro-ph/0106399.
- [50] For power spectrum $\ell^n C_\ell$, the choice of n is to an extent arbitrary. Our choices are conventional, but different values will shift the peak of the distributions in ℓ somewhat.
- [51] G. B. Poole, C. Blake, D. Parkinson, S. Brough, M. Colless, C. Contreras, W. Couch, D. J. Croton, S. Croom, T. Davis, et al., Mon. Not. Roy. Astron. Soc. **429**, 1902 (2013), arXiv:1211.5605 [astro-ph.CO].
- [52] A. Cimatti, R. Laureijs, B. Leibundgut, S. Lilly, R. Nichol, et al. (2009), arXiv:0912.0914 [astro-ph.CO].
- [53] G. C. Omer, Proc. Nat. Acad. Sci. **53**, 1 (1965).
- [54] Our approach is accurate during matter or Λ domination, but radiation will affect the accuracy at the largest distances. E.g., for $r > 0.97r_{\text{LS}}$, we have $\rho_{\text{rad}}/\rho_m > 0.1$ in the standard model. An early ISW effect is expected to modify our results slightly at the largest r values, where the constraints are strongest due to the SW effect.
- [55] J. P. Zibin and A. Moss, Class. Quant. Grav. **28**, 164005 (2011), arXiv:1105.0909 [astro-ph.CO].
- [56] J. P. Zibin, Phys. Rev. **D78**, 043504 (2008), arXiv:0804.1787 [astro-ph].
- [57] pla.esac.esa.int/pla/aio/planckProducts.html.
- [58] P. Ade et al. (Planck Collaboration) (2013), arXiv:1303.5077 [astro-ph.CO].
- [59] Refs. [69, 70] studied the detectability of voids against the CMB via lensing, but using the temperature anisotropies rather than the reconstructed lensing potential.
- [60] Note that this expected amplitude is only defined up to a constant factor of order unity, since it must depend on the shape of the structure's profile.
- [61] Note that the presence of such a structure outside surveys but inside our LSS *does* satisfy the Copernican principle: as we mentioned, most of our observable volume lies outside surveys, and, unless $R \simeq r_{\text{LS}}$, it is less likely for a structure to intersect our LSS than to be inside. E.g, if we have ~ 1 structure per today's observable volume, then it is most likely that such a structure would be outside surveys but not intersecting our LSS, and hence detectable only via CMB secondary effects.
- [62] G. Hinshaw, D. Larson, E. Komatsu, D. N. Spergel, C. L. Bennett, J. Dunkley, M. R.olta, M. Halpern, R. S. Hill, N. Odegard, et al., Astrophys. J. Suppl. **208**, 19 (2013), arXiv:1212.5226 [astro-ph.CO].
- [63] M. Kilbinger, L. Fu, C. Heymans, F. Simpson, J. Benjamin, T. Erben, J. Harnois-Déraps, H. Hoekstra, H. Hildebrandt, T. D. Kitching, et al., Mon. Not. R. Astron. Soc. **430**, 2200 (2013), arXiv:1212.3338 [astro-ph.CO].
- [64] E. F. Bunn, Phys. Rev. **D73**, 123517 (2006), arXiv:astro-ph/0603271.
- [65] R. Maartens, Phil. Trans. Roy. Soc. Lond. **A369**, 5115 (2011), arXiv:1104.1300 [astro-ph.CO].
- [66] J. R. Pritchard and A. Loeb, Rept. Prog. Phys. **75**, 086901 (2012), arXiv:1109.6012 [astro-ph.CO].
- [67] A. Lewis, A. Challinor, and A. Lasenby, Astrophys. J. **538**, 473 (2000), arXiv:astro-ph/9911177.
- [68] A. Lewis and S. Bridle, Phys. Rev. D **66**, 103511 (2002), arXiv:astro-ph/0205436.
- [69] S. Das and D. N. Spergel, Phys. Rev. **D79**, 043007 (2009), arXiv:0809.4704 [astro-ph].
- [70] I. Masina and A. Notari, JCAP **1009**, 028 (2010), arXiv:1007.0204 [astro-ph.CO].